

# Placenta Growth Factor in Diabetic Wound Healing

## *Altered Expression and Therapeutic Potential*

Francesca Cianfarani,\* Giovanna Zambruno,\*  
Laura Brogelli,\*† Francesco Sera,‡  
Pedro Miguel Lacal,¶ Maurizio Pesce,§  
Maurizio C. Capogrossi,† Cristina Maria Failla,\*  
Monica Napolitano,† and Teresa Odorisio\*

*From the Laboratorio di Biologia Molecolare e Cellulare,\*  
Laboratorio di Patologia Vascolare,† Laboratorio di Oncologia  
Molecolare,¶ Servizio di Epidemiologia,‡ Istituto Dermatologico  
dell'Immacolata, Istituto di Ricovero e Cura a Carattere  
Scientifico, Rome; and Laboratorio di Biologia Vascolare e  
Terapia Genica,§ Centro Cardiologico Monzino, Istituto di  
Ricovero e Cura a Carattere Scientifico, Milan, Italy*

**Reduced microcirculation and diminished expression of growth factors contribute to wound healing impairment in diabetes. Placenta growth factor (PlGF), an angiogenic mediator promoting pathophysiological neovascularization, is expressed during cutaneous wound healing and improves wound closure by enhancing angiogenesis. By using streptozotocin-induced diabetic mice, we here demonstrate that PlGF induction is strongly reduced in diabetic wounds. Diabetic transgenic mice overexpressing PlGF in the skin displayed accelerated wound closure compared with diabetic wild-type littermates. Moreover, diabetic wound treatment with an adenovirus vector expressing the human PlGF gene (*AdCMV.PlGF*) significantly accelerated the healing process compared with wounds treated with a control vector. The analysis of treated wounds showed that PlGF gene transfer improved granulation tissue formation, maturation, and vascularization, as well as monocytes/macrophages local recruitment. Platelet-derived growth factor, fibroblast growth factor-2, and vascular endothelial growth factor mRNA levels were increased in *AdCMV.PlGF*-treated wounds, possibly enhancing PlGF-mediated effects. Finally, PlGF treatment stimulated cultured dermal fibroblast migration, pointing to a direct role of PlGF in accelerating granulation tissue maturation. In conclusion, our data indicate that reduced PlGF expression contributes to impaired wound healing in diabetes and that**

**PlGF gene transfer to diabetic wounds exerts therapeutic activity by promoting different aspects of the repair process. (*Am J Pathol* 2006, 169:1167–1182; DOI: 10.2353/ajpath.2006.051314)**

Wound healing is a highly dynamic and complex process that can be divided into three main and partially overlapping phases: the early inflammatory, the intermediate proliferative, and the late tissue remodeling phases.<sup>1</sup> In diabetes, wound healing is defective, often resulting in ulcer formation. Numerous aspects of the wound repair process are altered in diabetes, including dysfunction in the inflammatory response, reduced granulation tissue formation, and impaired angiogenesis. The mechanisms underlying such defects are only partially understood. Among them, decreased growth factor production has been shown to play an important role.<sup>2</sup>

Neoangiogenesis of the granulation tissue, which transiently fills the wound bed reconstituting skin continuity, is a step occurring during the proliferative phase, necessary to sustain the metabolic demand and to allow the recruitment of inflammatory cells. Reduced vascularization strongly contributes to ulcer formation in diabetes,<sup>3</sup> and therapies aimed at enhancing angiogenesis have proved beneficial in accelerating diabetic wound closure. Different proangiogenic growth factors directly or indirectly mediate new vessel formation during skin repair. Among them, the placenta growth factor (PlGF), a member of the vascular endothelial growth factor (VEGF) family, plays an important role in promoting adult pathophysiological neovascularization and has been shown to contribute to wound healing by enhancing angiogenesis.<sup>4</sup> PlGF acts by

---

Supported by grants from the European Community (LSHB-CT-2005 512102) and the Italian Ministry of Health (Ricerca Corrente and Ricerca Finalizzata).

Accepted for publication July 11, 2006.

Supplemental material for this article can be found on <http://ajp.amjpathol.org>.

Address reprint requests to Teresa Odorisio, Ph.D., Laboratory of Molecular and Cell Biology, Istituto Dermatologico dell'Immacolata, IDI-IRCCS, Via dei Monti di Creta, 104, 00167 Rome, Italy. E-mail: t.odorisio@idi.it.

binding and activating the vascular endothelial growth factor receptor-1 (VEGFR-1)<sup>5</sup> and, in human, exists as four isoforms (PIGF-1, -2, -3, and -4) generated by alternative splicing that results in their different binding capability to heparin and the neuropilins.<sup>6-9</sup> PIGF promotes monocyte chemotaxis, collateral vessel growth, and bone marrow-derived precursor cell mobilization.<sup>10-12</sup> Some data indicate that PIGF may have a direct action on endothelial cells mediated by VEGFR-1 receptor binding.<sup>13</sup> However, *in vivo* experimental findings show that PIGF angiogenic potential also relies on the potentiation of VEGF activity.<sup>4</sup>

Based on its role in adult angiogenesis, PIGF has been regarded as an attractive candidate for the therapeutic modulation of adult angiogenesis, and studies on heart and hindlimb ischemia animal models have confirmed the therapeutic potential of PIGF administration.<sup>11,14,15</sup>

*In vivo*, PIGF exerts a strong angiogenic activity. Transgenic mice overexpressing PIGF under the keratin 14 promoter (K14-PIGF mice) exhibit a robust increase in dermal vascularization that is formed of markedly enlarged and also more numerous and permeable vessels.<sup>16</sup> In keeping with this finding, adeno-mediated PIGF gene transfer in the skin is able to elicit a strong angiogenic response, giving rise to more numerous and strikingly larger vessels.<sup>14</sup> PIGF gene transfer does not affect lymphatic vasculature and induces blood vessel permeability only when high adenovirus concentrations are used.<sup>17,18</sup>

In adult skin, PIGF expression is barely detectable, and it is up-regulated in association with both physiological and pathological neoangiogenesis, such as in the hair follicle cycle,<sup>19</sup> during wound healing,<sup>20</sup> and in melanoma cells.<sup>21,22</sup> During the angiogenic phase of wound healing, PIGF is expressed by migrating keratinocytes and endothelial cells of small blood vessels, acting in a paracrine and autocrine way on VEGFR-1-expressing endothelium.<sup>20</sup> Moreover, lack of PIGF results in delayed wound closure, indicating that this factor is required for optimal skin repair.<sup>4</sup>

By using streptozotocin-induced diabetic mice, a mouse model of type-1 diabetes, we investigated whether PIGF may be involved in the healing impairment of diabetic cutaneous wounds. We also evaluated the activity of adenovirus-mediated PIGF gene transfer in promoting diabetic skin repair.

## Materials and Methods

### Mice

C57Bl/6 mice were purchased from Charles River (Calco, Italy). Transgenic mice overexpressing PIGF under the control of the human keratin 14 promoter (K14-PIGF mice) have a BDF1 background and have been produced and phenotypically characterized in our laboratory.<sup>16</sup>

### Adenovirus Vectors

The full cDNA for the human PIGF-1 isoform<sup>6</sup> was inserted into the pAdTrack-constitutive cytomegalovirus (CMV) expression vector (Stratagene, La Jolla, CA) under the control of the CMV immediate-early promoter/enhancer. The pAdTrack-CMV plasmid contains the gene for the green fluorescent protein (GFP) under the control of a second CMV promoter and sequences for homologous recombination with the replication-deficient serotype 5 adenovirus (Ad5). The plasmid containing the human PIGF-1 was linearized and transformed with the pADEasy-1 plasmid (Stratagene) in BJ5138 *Escherichia coli* cells. The pAdCMV.PIGF, obtained following homologous recombination between pAdTrack-CMV.PIGF and pADEasy-1, was selected for its resistance to kanamycin and sequenced to check the recombination event.

The control vector, carrying the cDNA for the *E. coli* LacZ gene and coding for the enzyme  $\beta$ -galactosidase (AdCMV.LacZ), was obtained following the same procedure.

AdCMV.PIGF and AdCMV.LacZ were propagated in 293 cells (American Type Culture Collection, Manassas, VA), modified to constitutively express viral genes for the formation of viral particles deleted in the pADEasy-1 vector, and were purified by a CsCl density gradient. The preparation was dialyzed and stored in dialysis buffer (10 mmol/L Tris-HCl and 1 mmol/L MgCl<sub>2</sub>, pH 7.4) with 10% glycerol at  $-70^{\circ}\text{C}$ . The titer of viral stocks was determined by plaque assay in 293 cells.

### Diabetic Wound Model and Wound Closure Analysis

Five-week-old C57Bl/6 male mice were rendered diabetic by a single intraperitoneal injection of 180 mg/kg streptozotocin (Sigma-Aldrich, St. Louis, MO). After 7 days, glucose level was measured in the peripheral blood, and mice with glycemia over 250 mg/dl were selected for the study. Two weeks later, the dorsum of anesthetized diabetic mice and age-matched healthy controls was shaved, and a 6 mm-diameter full-thickness wound was performed on the dorsal midline using a biopsy punch. One day after injury, the wounds of diabetic mice were treated with 50  $\mu\text{l}$  of saline solution alone or containing  $5 \times 10^8$  pfu of AdCMV.PIGF or  $5 \times 10^8$  pfu of AdCMV.LacZ, delivered with a Hamilton's syringe under the clot covering the wound. The wound area of healthy controls was treated with an equivalent volume of saline solution. The wound margin was traced on a transparency film put on the back of treated mice immediately after wounding (day 0) and every 2nd day thereafter (days 2, 4, 6, etc. after wounding, corresponding to day 1, 3, 5, etc. after treatment). A blinded operator measured traced areas of the wounds using a computer-assisted image analyzer (KS300; Zeiss, Jena, Germany). The rate of healing was expressed as the percentage of the area at day 0. Sixteen to 22 animals/group were analyzed as a total of three independent experiments.

Eight- to 10-week-old transgenic mice and wild-type littermates were used for the analysis of K14-PIGF mice. Diabetes induction, wounds, and closure analysis were performed on groups of nine animals as described above, apart from the timing of wound closure analysis that was performed every 2nd or 3rd day.

### *Reverse Transcriptase-Polymerase Chain Reaction (RT-PCR) and Real-Time RT-PCR*

Cultured human dermal fibroblasts, human umbilical vein endothelial cells, HaCaT cells, and wounds with surrounding normal skin were homogenized in TRIzol (Life Technologies, Invitrogen, Groningen, The Netherlands) and total RNA extracted and purified following the manufacturer's instructions. RNA was converted into cDNA using the first Strand cDNA Synthesis Kit (Roche Bioproducts, Basel, Switzerland). The cDNAs were used as templates in RT-PCR or real-time RT-PCR. For RT-PCR of VEGFR-1 and VEGFR-2, the following primers were used: VEGFR-1 forward (5'-CTCCTGAGTACTCTACTCCT-3') and reverse (5'-GAGTACAGGACCACCGAGTT-3'), amplifying a 632-bp fragment, and VEGFR-2 forward (5'-GTCTATGCCATTCTCCCCC-3') and reverse (5'-GAGACAGCTTGGCTGGGCT-3'), amplifying a cDNA fragment of 85 bp.

For real-time RT-PCR, the SYBR Green PCR Master Mix (Applied Biosystem, Foster City, CA) was used following the manufacturer's instructions, and the following gene-specific primers were designed using the Primer Express software (Applied Biosystems): PIGF forward (5'-GTGTGCCGATAAAGACAGCCA-3') and reverse (5'-GAAATGTGGATCCCGATTGG-3'); VEGF forward (5'-GTGCAGGCTGCTGTAACGAT-3') and reverse (5'-GCA-TGATCTGCATGGTGATGTT-3'); VEGFR-1, transmembrane form, forward (5'-AAACTAGGCAAATCGCTCGG-3') and reverse (5'-GGCTTGAACGACTTTCCCAA-3'); and VEGFR-1, soluble form, forward (5'-TCAGGCCAG-AGGAAAGC-3') and reverse (5'-GAGGGCACTGGGCT-TTCTTA-3'). For the transforming growth factor  $\beta$ -1 (TG- $\beta$ -1), fibroblast growth factor-2 (FGF-2), and platelet-derived growth factor-B (PDGF-B), the forward and reverse primers reported by Galiano et al<sup>23</sup> were used.

Gene-specific PCR products were measured by means of the ABI PRISM 5700 detection system (Perkin-Elmer, Norwalk, CT) and normalized to the glycer-aldehyde-3-phosphate dehydrogenase (GAPDH) amplification obtained with specific primers (forward-5'-GTATGACTC-CACTCACGGCAAAA-3' and reverse-5'-TTC-CCATTCTC-GGCCTTG-3'). Quantification was performed using the comparative CT method.<sup>24</sup> A non-template control was run with every assay by adding water in place of cDNA, and all determinations were performed in triplicate.

### *Enzyme-Linked Immunosorbent Assay (ELISA)*

Protein extracts from skin wound biopsies were obtained as described.<sup>16</sup> Plasma samples used for the detection of human PIGF were obtained from blood collected from the jugular vein using a syringe containing an anticoag-

ulant (Liquemin, 100,000 u.i.; Roche Bioproducts). Blood was immediately transferred in a vial containing EDTA at a concentration of 1.6 mg/ml and mixed with an equal volume of PBS without calcium and magnesium. After adding 3 vol of Lymphoprep (Axis-Shield PoC As, Oslo, Norway) to the mixture, a discontinuous density gradient was obtained by centrifugation, and the upper phase containing the plasma was collected.

Mouse PIGF and VEGF were quantified in wound extracts of diabetic and healthy mice using specific murine Quantikine ELISA Kit (R&D Systems, Abingdon, UK), following the manufacturer's instructions. Human PIGF was detected in wound extracts after AdCMV.PIGF, AdCMV.LacZ, or saline local application or in plasma samples by using Quantikine human PIGF ELISA kit (R&D Systems). VEGFR-1 was quantified in 96-well plates coated with 50  $\mu$ l of an anti-mouse VEGFR-1 antibody (AF471; R&D Systems) at a concentration of 10  $\mu$ g/ml overnight at room temperature. The plates were then washed and incubated for 2 hours with 3% bovine serum albumin in PBS. After washing, 80  $\mu$ g of protein extracts from diabetic and healthy mouse wounds were added to the plates for 2 hours at room temperature, followed by a 2-hour incubation with biotinylated anti-mouse VEGFR-1 antibody (BAF471; R&D Systems). The plates were then incubated overnight with horseradish peroxidase-conjugated streptavidin, diluted 1:1000. Colorimetric reactions were read at 490 nm in a Microplate Reader 3550-UV (Bio-Rad, Life Science Group, Hercules, CA).

### *Analysis of GFP Expression*

Wounds surrounded by normal skin were dissected 1 day after adenovirus application and frozen in Tissue-Tek OCT Compound (Sakura Finetek, Torrance, CA). Ten- $\mu$ m cryostat sections were obtained and immediately analyzed at the fluorescence microscope.

### *In Situ Hybridization*

Paraformaldehyde-fixed, paraffin-embedded wound specimens were processed as previously described.<sup>20</sup> The mouse PIGF riboprobe containing the entire coding sequence and the human PIGF riboprobe spanning the cDNA region common to all of the human PIGF isoforms were previously described.<sup>16,20</sup>

### *Immunohistochemistry*

Four- $\mu$ m-thick paraformaldehyde-fixed, paraffin-embedded sections from skin biopsies containing the wounds were processed as described.<sup>20</sup> To detect endothelial cells, an anti-mouse platelet endothelial cell adhesion molecule-1 (PECAM/CD31) polyclonal antibody (M 20; Santa Cruz Biotechnology, Santa Cruz, CA) was used at a concentration of 1  $\mu$ g/ml for 14 hours at 4°C following antigen retrieval with a microwave treatment at 650 W for 2 plus 5 minutes. Smooth muscle cells/pericytes surrounding blood vessels were stained by using a mouse monoclonal anti- $\alpha$ -smooth muscle actin (clone 1A4;

DakoCytomation, Milan, Italy) diluted 1:50, for 1 hour at room temperature after antigen retrieval in microwave at 650 W for 3 minutes using the Dakoark kit (DakoCytomation). Monocytes/macrophages were identified with an anti-mouse monoclonal antibody (Mac3, clone M3/84; PharMingen, BD Biosciences, Franklin Lakes, NJ) at a concentration of 5  $\mu\text{g}/\text{ml}$  for 2 hours at room temperature after microwave treatment at 600 W for 3 minutes. Human PIGF was detected using an anti-goat polyclonal antibody (C-20; Santa Cruz Biotechnology) as described.<sup>20</sup> Negative controls were obtained by omitting the primary antibody.

### *Computer-Assisted Morphometric Analysis*

Two blinded observers independently analyzed granulation tissue area, CD31-positive vessel density and area,  $\alpha$ -smooth muscle actin-positive vessel density, and Mac3-positive cell density by computer-assisted image analysis using a Zeiss KS300 Version 3.0 program. CD31-positive vessel density and area,  $\alpha$ -smooth muscle actin-positive vessel density, and Mac3-positive cell density were calculated on 8 to 12 noncontiguous, randomly selected fields within the granulation tissue at  $\times 100$  magnification.

### *Colony-Forming Assay of Isolated Myeloid Precursors*

Peripheral blood mononuclear cells (PBMC) were isolated from heparinized blood after centrifugation over a discontinuous gradient using Lymphoprep (Axis-Shield PoC As). After centrifugation, PBMC present in the intermediate phase were resuspended in Iscove modified Dulbecco's medium (Gibco, Invitrogen). PBMC were seeded at a density of  $1.2 \times 10^5$  cells/well in six multi-well plates containing methyl-cellulose culture medium (Methocult; StemCell Technologies, Grenoble, France) and the number of colonies/well was counted after 2 weeks of culture.

### *Cell Cultures*

Primary human fibroblast cultures previously established from skin biopsies from healthy volunteers were grown in F10 medium supplemented with 10% fetal calf serum. The human keratinocyte cell line HaCaT was maintained in Dulbecco's modified Eagle's medium supplemented with 10% fetal calf serum and 4 mmol/L glutamine. Human umbilical vein endothelial cells were isolated from freshly delivered umbilical cords as previously described<sup>25</sup> and cultured in Endothelial Cell Growth Medium-2 kit from Clonetics (BioWhittaker Inc., Walkersville, MD).

### *Western Blot*

Semiconfluent normal human fibroblasts were lysed and boiled in SDS sample buffer (50 mmol/L Tris-HCl,

pH 6.8, 100 mmol/L dithiothreitol, 2% SDS, 0.1% bromophenol blue, and 10% glycerol). Equal amounts of protein per sample were analyzed in 7 or 10% SDS-polyacrylamide gels. Proteins were then transferred to nitrocellulose membranes (Hybond-C; Amersham Life Science, Buckinghamshire, UK), using a Transblot apparatus (Bio-Rad). Membranes were blocked in blocking solution (2% nonfat dry milk, 1% Triton X-100, 10 mmol/L EDTA, and 50 mmol/L Tris-HCl, pH 7.5) and incubated overnight at 4°C with the primary antibody, diluted in blocking solution. The anti-VEGFR-1 rabbit polyclonal antibody (C-17; Santa Cruz Biotechnology) was used at 2  $\mu\text{g}/\text{ml}$ , the anti-VEGFR-2 goat polyclonal antibody (AF357; R&D Systems) was used at 0.2  $\mu\text{g}/\text{ml}$ , and the anti- $\beta$ -actin monoclonal antibody (AC-40; Sigma-Aldrich) was diluted 1:1000. After washing twice with blocking solution, membranes were incubated for 1 hour at room temperature with the secondary antibody (anti-rabbit or anti-mouse Ig/horseradish peroxidase, Amersham Life Science; or anti-goat Ig/horseradish peroxidase, Sigma-Aldrich; all diluted 1:5000 in blocking solution). Membranes were then washed with 0.1% Tween 20/TBS, and detection was performed using the ECL Western blotting detection reagents (Amersham Life Science).

### *Migration Assay*

Fibroblast migration was analyzed using Boyden chambers (Neuroprobe Inc., Gaithersburg, MD) equipped with 8- $\mu\text{m}$  pore diameter polycarbonate filters (Nuclepore; Whatman Incorporated, Clifton, NJ) coated with 5  $\mu\text{g}/\text{ml}$  of a gelatin solution. In brief, cells were suspended in migration medium (1  $\mu\text{g}/\text{ml}$  heparin/0.1% bovine serum albumin in DMEM) and loaded ( $2 \times 10^5$  cells) into the upper compartment of the Boyden chambers. Migration medium containing grading concentrations of human recombinant PIGF (10 to 100 ng/ml/hour PIGF-1; from R&D Systems) was added to the lower compartment of the chambers. After 16 hours incubation at 37°C in a CO<sub>2</sub> incubator, the filters were removed from the chambers, fixed in 4% paraformaldehyde/PBS, and stained with 0.5% crystal violet. The cells from the upper surface of the filter were removed by wiping with a cotton swab, and the filters were mounted on a slide. Migrated cells, attached to the lower surface of the filters, were then counted under the microscope. Ten (50 $\times$ ) magnification microscopic fields randomly selected on each filter were scored for each experimental condition. Experiments were performed in triplicate. Basal migration was determined by including migration medium in the lower compartment of the Boyden chambers, while as a positive control, cell migration stimulated by a mixture of insulin-transferrin-sodium selenite (Sigma-Aldrich) was analyzed. To verify the specificity of the observed effect, PIGF was incubated in the presence of 10  $\mu\text{g}/\text{ml}$  of its blocking antibody (MAB 264; R&D Systems) or of an antibody blocking VEGF (MAB 293; R&D Systems). To evaluate the involvement of VEGFR-1 and VEGFR-2 in mediating PIGF-induced fibroblast migration, cells were

seeded in the presence of 10  $\mu\text{g/ml}$  of an anti-VEGFR-1 (AF 321; R&D Systems) or an anti-VEGFR-2 (AF 357; R&D Systems) antibody.

### Proliferation Analysis

Fibroblast proliferation was determined using the bromodeoxyuridine method (Cell Proliferation ELISA, BrdU colorimetric kit; Roche) in 96-well tissue culture plates in triplicate. Fibroblasts (4000 cells/well) were seeded and cultured in F10 medium containing 10% FCS. After 10 hours, medium was removed, and cells were maintained overnight in medium containing 0.1% bovine serum albumin (starving condition). Cells were then treated with F10 medium containing 0.1% bovine serum albumin, a mixture of insulin-transferrin-sodium selenite (Sigma-Aldrich), diluted 1:100, and heparin (Sigma-Aldrich) without (negative control) or in the presence of 10 ng/ml FGF-2 (234-FSE; R&D Systems), used as positive control, or of PIGF at a concentration of 10, 20, 50, or 100 ng/ml. The cell number was determined at 0, 24, 48, and 72 hours after the addition of PIGF. Twelve hours prior proliferation analysis, bromodeoxyuridine was added to the medium. Cell proliferation was then calculated by determining bromodeoxyuridine incorporation with an ELISA assay, following manufacturer's instructions.

### Statistical Analysis

Numerical differences were analyzed by using the two-tailed Student's *t*-test. *P* values less than 0.05 were considered significant. For the wound closure analysis, the six pairwise differences of the wound area between treatment groups (AdCMV.PIGF, AdCMV.LacZ, and saline solution) and healthy controls were tested using the two-tailed Student's *t*-test. The analysis of variance for repeated measures (split-plot design) was also applied to test the treatment interaction with time and to derive, using the Tukey procedures for multiple comparisons, the estimate of wound area differences (95% confidence interval) within each pair of treatments.

## Results

### PIGF Expression Is Strongly Reduced in the Wounds of Diabetic Mice

PIGF mRNA levels were analyzed by real-time RT-PCR on RNA extracted from skin-punch biopsies containing the wounds, taken at different time points after injury, from diabetic and healthy control mice (Figure 1A). In healthy animals PIGF mRNA induction started at day 1 and reached a peak at day 3, concomitantly with the initiation of granulation tissue formation. PIGF mRNA levels remained higher than those present in unwounded skin at least up to day 9. In diabetic mice, PIGF mRNA induction

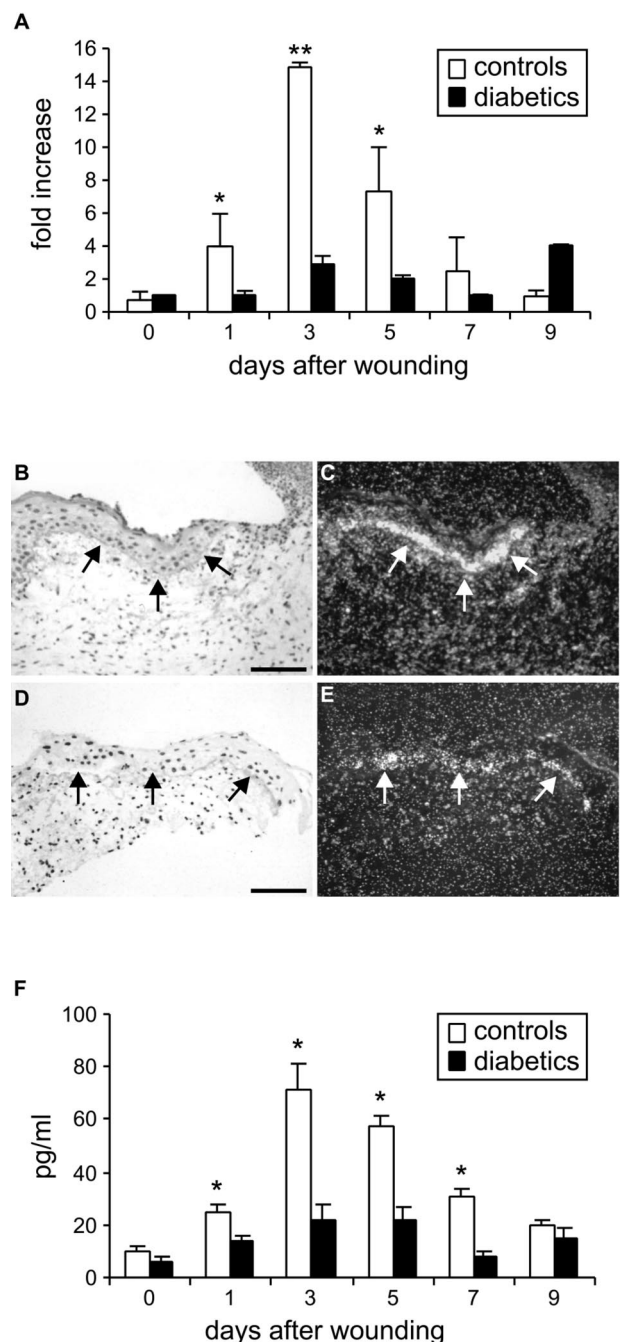


**Figure 1.** Expression of PIGF in the diabetic wounds. **A:** Real-time PCR analysis of mouse PIGF mRNA levels during wound healing shows that the induction of PIGF is strongly reduced in diabetic mice compared with healthy controls. Results are expressed as relative fold induction versus PIGF expression at day 0 in diabetic mice ( $n = 3$ ). \* $P < 0.05$ ; \*\* $P < 0.01$ . **B–E:** *In situ* hybridization on wound specimens taken at day 3 after injury shows that migrating keratinocytes at the wound margin (**arrows**) display reduced PIGF mRNA levels in the wounds of diabetic mice (**D, E**) with respect to healthy animals (**B, C**). **B, D:** bright field; **C, E:** dark field. Scale bars = 75  $\mu\text{m}$ . **F:** ELISA for mouse PIGF measurement in protein extracts of healthy and diabetic wounds shows the reduction in PIGF protein in diabetic wounds. \* $P < 0.05$ .

was strongly reduced compared with healthy controls, reaching a fivefold difference ( $2.82 \pm 0.43$  in diabetics versus  $14.85 \pm 0.33$  in healthy mice) at day 3.

By *in situ* hybridization analysis using a mouse PIGF riboprobe on wound specimens collected at day 3, a strong signal was detected on migrating keratinocytes at the wound margin in healthy control animals (Figure 1, B and C). In diabetic wounds, the hybridization signal on keratinocytes was visible but much weaker compared with controls (Figure 1, D and E).

The analysis by ELISA indicated that PIGF induction was also strongly reduced at the protein level in diabetic wounds (Figure 1F). In control mice PIGF started to increase at day 1, reached the highest levels at day 3, and remained up-regulated at least until day 9. In diabetic wounds, PIGF induction was evident but significantly reduced with respect to nondiabetic controls from day 1 to day 7, with an almost 3.5-fold difference ( $21.83 \pm 5.67$  versus  $71.07 \pm 9.8$  pg/ml) at day 3.

VEGF expression was also analyzed by real-time RT-PCR on the same extracts used for PIGF mRNA detection. As expected, VEGF mRNA expression was induced in healthy wounds, with a peak at day 3 after wounding. In diabetic samples VEGF mRNA levels were reduced compared with healthy controls at all of the time points analyzed, reaching a more than three-fold difference at day 3 and day 5 after wounding (Supplementary Figure 1, see <http://ajp.amjpathol.org>).

In parallel, we also verified whether the decrease in PIGF expression correlates with reduced VEGFR-1 levels, by real-time RT-PCR and ELISA. VEGFR-1 mRNA can be differently processed to give rise to a membrane or a soluble form, the latter lacking the intracellular and transmembrane domains and containing a unique sequence at the 3' end.<sup>26</sup> The soluble form is considered to negatively act on angiogenesis by interfering with growth factor binding to the transmembrane tyrosine kinase receptor. The mRNA analysis was, therefore, performed using two different sets of primers, one recognizing the intracellular region, thus amplifying the cDNA for the transmembrane form, and a second one amplifying 72 nucleotides localized in the sequence specific for the soluble form. By using both sets of primers, a decreased amount of mRNA coding for VEGFR-1 was detected in the diabetic wounds compared with healthy controls at all of the time points analyzed (up to 9 days after wounding). In particular, the mRNA for the membrane receptor was significantly reduced at day 9 after injury in diabetic wounds, with an almost threefold difference compared with healthy wounds ( $1.39 \pm 0.28$ - versus  $3.91 \pm 1.13$ -fold increase over diabetic wound at day 1) (Figure 2A). The selective amplification of the mRNA transcript encoding for the soluble form revealed a marked decrease in the diabetic wounds at day 3, 7, and 9, the difference being of about threefold at day 7 ( $2.64 \pm 0.84$ - versus  $7.84 \pm 1.7$ -fold increase over diabetic wound at day 1) (Figure 2B). The ELISA for mouse VEGFR-1 indicated that also at the protein level, the expression was decreased in diabetic wounds, the differences between diabetic wounds and healthy controls, expressed as fold increase over diabetic wound at day 0, being significant at days 7 and 9 after wounding (Figure 2C).

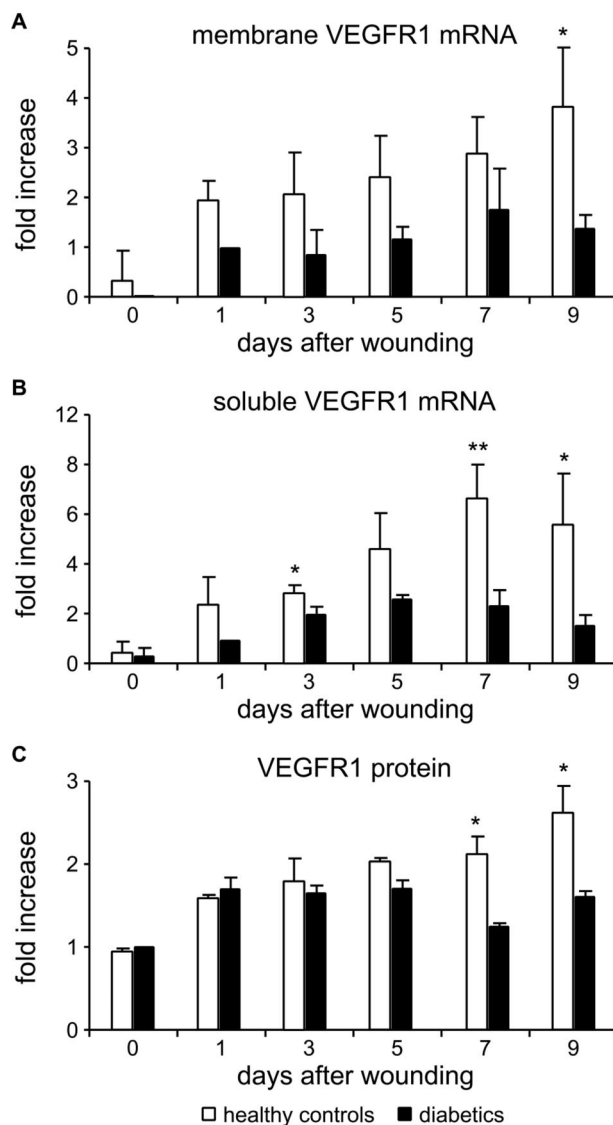


**Figure 2.** Expression of VEGFR-1 in the diabetic wounds. **A** and **B**: Real-time RT-PCR analysis with primers amplifying the mRNAs encoding the membrane VEGFR-1 (**A**) or the sequence specific for the soluble form (**B**) indicates that the induction of both isoforms is decreased in diabetic wounds compared with healthy controls. Results are expressed as relative fold induction versus VEGFR-1 mRNA expression at day 1 in diabetic mice ( $n = 3$ ), because at day 0, the amplified sequence of the membrane isoform (**A**) was undetectable in the diabetic samples. \* $P < 0.05$ ; \*\* $P < 0.01$ . **C**: ELISA for VEGFR-1 confirming the reduction at the protein level in the expression of the PIGF receptor in diabetic mice. Results are expressed as relative fold induction versus VEGFR-1 expression at day 0 in diabetic mice ( $n = 3$ ). \* $P < 0.05$ .

### Wound Healing Is Accelerated in Diabetic K14-PIGF Transgenic Mice

To verify whether high levels of keratinocyte-derived PIGF are able to rescue the healing impairment characteristic of diabetes, wound healing was monitored up to complete closure in transgenic mice overexpressing PIGF under the control of the keratin 14 promoter (K14-PIGF mice), rendered or not diabetic by streptozotocin treatment. Wound closure occurred 14 days after injury both in K14-PIGF mice and wild-type controls in basal

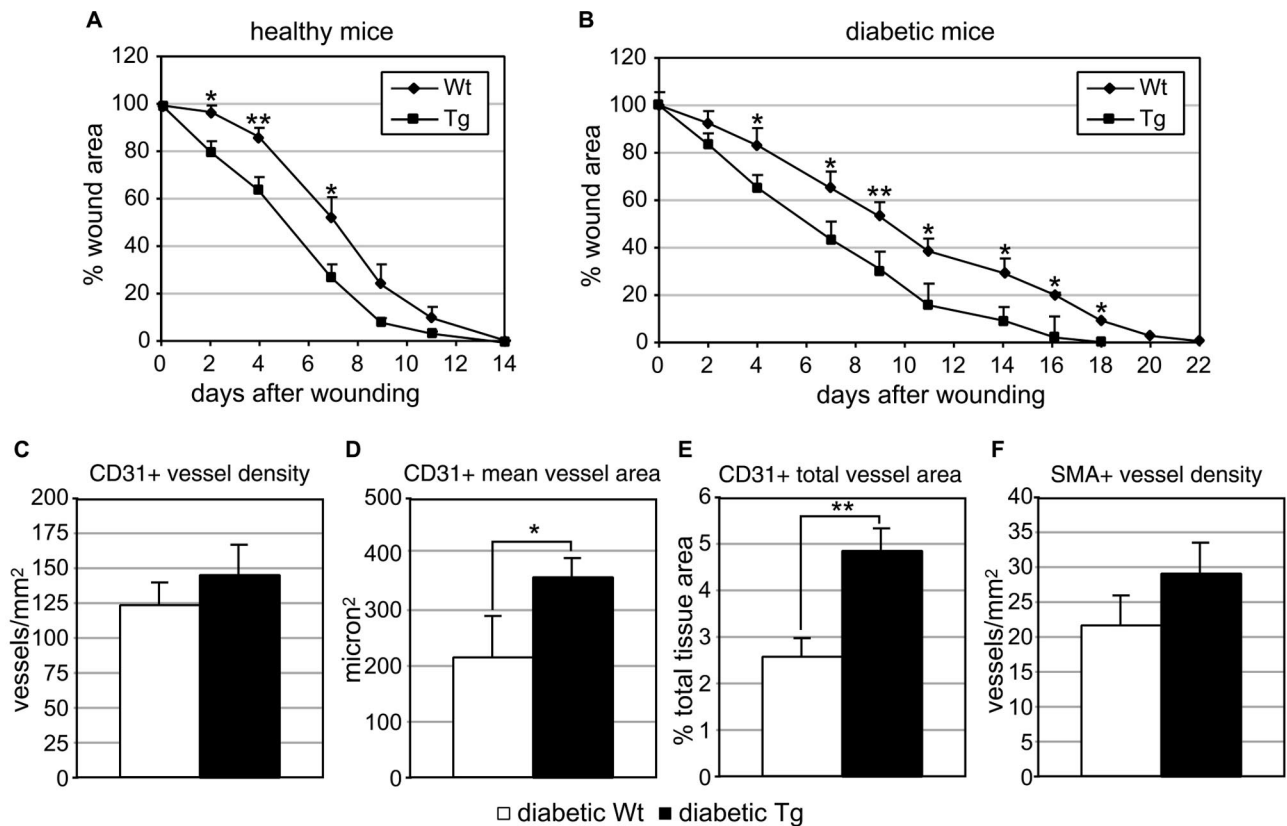


**Figure 3.** Analysis of wound closure in transgenic mice overexpressing PIGF in the skin (K14-PIGF mice). **A:** In K14-PIGF transgenic mice, wound closure is not accelerated compared with nontransgenic littermates, but the wound area is significantly reduced at early time points (2, 4, and 7 days after wounding) ( $n = 9$ ). **B:** In diabetic K14-PIGF transgenic mice, wound closure is accelerated compared with diabetic nontransgenic littermates (18 versus 22 days), with a significant reduction in the wound area starting from day 4 and up to wound closure ( $n = 9$ ).  $*P < 0.05$ ;  $**P < 0.01$ . **C–F:** Analysis of granulation tissue vascularization in diabetic K14-PIGF mice and diabetic wild-type littermates. Central sections of wounds collected at day 7 after injury were stained with an anti-PECAM/CD31 antibody or an anti- $\alpha$ -smooth muscle actin (SMA) antibody to detect endothelial cells and pericytes/smooth muscle cells, respectively. Vessel density (**C**, **F**), mean vessel area (**D**), and percentage area covered by vessels (**E**) were measured by computer-assisted morphometric analysis. K14-PIGF mice showed increased vascularization for all of the parameters analyzed compared with nontransgenic controls, but the differences were significant only for the CD31<sup>+</sup> main vessel area (**D**) and total area covered by vessels (**E**) ( $n = 6$ ). Values are expressed as mean  $\pm$  SEM.  $*P < 0.05$ ;  $**P < 0.01$ .

conditions (ie, in the absence of diabetes) (Figure 3A). An improvement of the healing process was evident in transgenic mice at all time points analyzed compared with wild-type littermates, with a significant decrease in the wound area at the early time points (days 2, 4, and 7). Wound healing was then analyzed in diabetic mice. Wound closure was accelerated in K14-PIGF diabetic mice (18 days) compared with control diabetic littermates (22 days), with a significant reduction of the wound area starting from day 4 and up to day 18 (Figure 3B).

The biological effect of the constitutive PIGF overexpression in the diabetic wounds was also characterized. Granulation tissue extension and vascularization were analyzed by computer-assisted morphometric analysis in central wound sections from diabetic transgenic mice and diabetic wild-type littermates collected at day 7 after injury. This analysis indicated that in K14-PIGF diabetic mice granulation tissue formation was increased, despite not significantly ( $2.67 \pm 1.09$  mm<sup>2</sup> in wild-type mice versus  $3.21 \pm 0.67$  mm<sup>2</sup> in K14-PIGF mice) (data not shown). Vascularization was analyzed by staining vessels with an anti-PECAM/CD31 antibody to detect blood endothelial cells or with

an anti- $\alpha$ -smooth muscle actin (SMA) antibody recognizing vessels surrounded by pericytes/smooth muscle cells. This analysis revealed an increase, although not statistically significant, in vessel density after immunostaining with both antibodies (Figure 3, C and F) and showed that the mean vessel area as well as the total area of PECAM/CD31-positive vessels were significantly augmented in the granulation tissue of K14-PIGF mice compared with wild-type controls (Figure 3, D and E). PIGF is a strong chemoattractant for VEGFR1<sup>+</sup> monocytes/macrophages.<sup>10</sup> Therefore, we investigated whether the increased PIGF expression in K14-PIGF diabetic wounds correlates with enhanced monocyte/macrophage recruitment at the wound site. Wound sections were stained with an antibody against the Mac3 antigen that is expressed on mouse monocytes and activated macrophages, and the number of labeled cells within the granulation tissue quantified by computer-assisted morphometric analysis. The results indicated that monocyte/macrophage number was comparable in diabetic K14-PIGF mice and their diabetic controls ( $596 \pm 67$ /mm<sup>2</sup> in wild-type mice versus  $622 \pm 79$ /mm<sup>2</sup> in K14-PIGF mice) (data not shown).

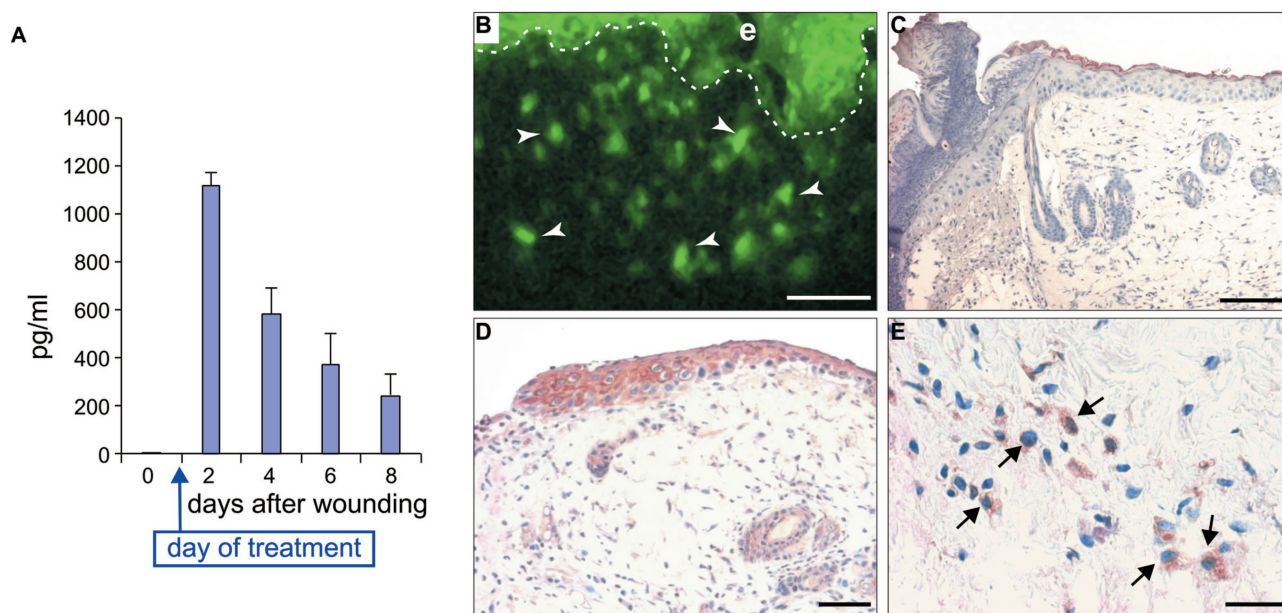


**Figure 4.** Efficacy of AdCMV.PIGF transfer into the wounds. **A:** ELISA for human PIGF of proteins extracted from AdCMV.PIGF-treated wounds dissected at different times after injury. **B:** GFP analysis of an AdCMV.PIGF-treated diabetic wound taken 1 day after treatment showing homogeneous fluorescence throughout the epidermis (e) and numerous positive cells in the dermis (arrows). Scale bar = 50  $\mu$ m. **C–E:** Immunohistochemistry for human PIGF in wounds collected 1 day after treatment from AdCMV.LacZ-treated- (C) and AdCMV.PIGF-treated diabetic wounds (D and E). Staining is detectable in different cells in AdCMV.PIGF-treated wounds, both in the epidermis and in the dermis (D), whereas AdCMV.LacZ-treated wounds do not show any specific staining for human PIGF (C). **E:** Higher magnification of D showing positive cells in the dermis (arrows) of AdCMV.PIGF-treated mice. Scale bars: C, D, 50  $\mu$ m; E, 25  $\mu$ m.

### Topical Administration of an Adenovirus Carrying the Human PIGF-1 Results in High PIGF Expression at the Wound Site

To test the potential therapeutic effect of PIGF administration in diabetic wound healing, an adenovirus vector containing the cDNA for the human PIGF-1 isoform (AdCMV.PIGF) or for the LacZ gene (AdCMV.LacZ) was topically applied 1 day after injury on excisional wounds performed in diabetic mice. We first verified whether AdCMV.PIGF efficiently transduced PIGF at the wound site. To this end, human PIGF expression was analyzed by ELISA on protein extracts obtained from the wounds at various times after injury (Figure 4A). This analysis revealed that the day after AdCMV.PIGF application (ie, day 2 after wounding) adenovirus-derived PIGF was actively expressed in the wounds. Thereafter, human PIGF expression progressively decreased but persisted at high levels at least up to 1 week after adenovirus administration. As expected, human PIGF was undetectable in AdCMV.LacZ-treated wounds at all time points analyzed (not shown).

As AdCMV.PIGF contains the GFP gene, we analyzed under the fluorescence microscope the extent of adenovirus-mediated gene transfer in the treated wounds. The analysis of wound specimens excised 1 day after adenovirus application revealed numerous GFP-positive cells at the wound margin in AdCMV.PIGF-treated wounds, including keratinocytes and cells located in the dermis (Figure 4B). *In situ* hybridization analysis performed on wound tissue specimens collected the day after treatment indicated that different cell types, comprising epidermal keratinocytes, cells located in the der-

mis and in the panniculus carnosus, transcribed human PIGF following adenovirus infection (data not shown). No specific hybridization signal could be detected on specimens from AdCMV.LacZ-treated wounds. Immunohistochemistry with an anti-human PIGF antibody on the same specimens confirmed that adenovirus-derived PIGF expression was widely distributed within the wounds of AdCMV.PIGF-treated mice but not in AdCMV.LacZ-treated controls (Figure 4, C–E).

### AdCMV.PIGF Treatment Accelerates Cutaneous Wound Closure in Diabetic Mice

To test the effect of AdCMV.PIGF topical treatment in diabetic wound healing, excisional punch biopsies were performed in diabetic and healthy control mice and diabetic wounds were treated with  $5 \times 10^8$  pfu of AdCMV.PIGF or with  $5 \times 10^8$  pfu of AdCMV.LacZ or with saline solution. The analysis of wound closure indicated that all healthy controls healed by day 18 (Figure 5A). All diabetic wounds treated with saline healed by day 26, as did AdCMV.LacZ-treated wounds. In contrast, all diabetic wounds treated with AdCMV.PIGF healed by day 20. The analysis of the wound area measured every second day after injury (ie, days 1, 3, 5, etc. after treatment) revealed a significant reduction in AdCMV.PIGF-treated mice compared with AdCMV.LacZ-treated mice, starting from day 6 and up to wound closure (Figure 5, A and B) (test for interaction treatment with time,  $P < 0.0001$ ). No significant difference in the wound area could be observed at any time point analyzed neither between healthy controls and AdCMV.PIGF-treated diabetic wounds nor between AdCMV.LacZ- and saline-treated diabetic wounds.



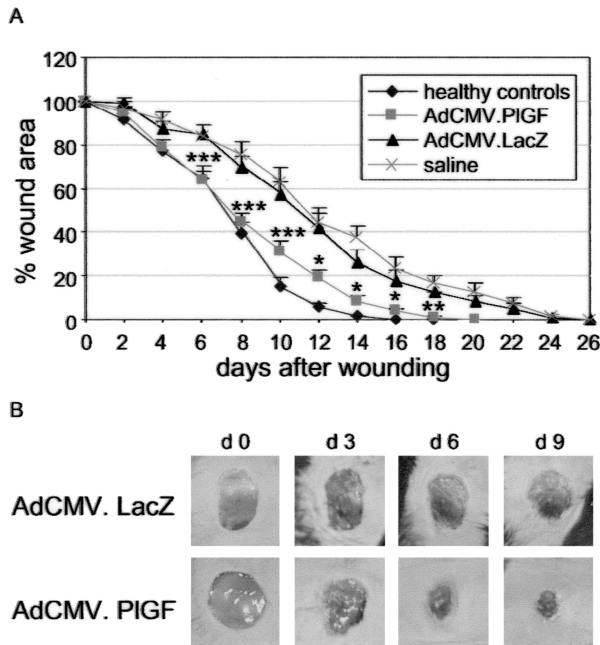


**Figure 5.** Wound closure analysis in diabetic mice treated with AdCMV.PIGF and in controls. **A:** Topical application of AdCMV.PIGF accelerates wound closure in diabetic mice with respect to saline and AdCMV.LacZ treatments, approximating the timing of closure observed in untreated healthy controls. The wound area is significantly reduced in AdCMV.PIGF-treated diabetic mice compared with AdCMV.LacZ- and saline-treated diabetic mice but not with untreated healthy animals. \* $P < 0.05$ ; \*\* $P < 0.01$ ; \*\*\* $P < 0.005$ , AdCMV.PIGF versus AdCMV.LacZ. **B:** Representative pictures of diabetic wounds treated either with AdCMV.PIGF or with AdCMV.LacZ taken immediately after wounding (day 0) and at different times after injury, illustrating the increased reduction of the wound area following PIGF gene transfer compared with LacZ gene transfer.

### *AdCMV.PIGF Treatment Associates with Increased Formation and Accelerated Maturation of the Granulation Tissue*

To characterize the biological effects underlying AdCMV.PIGF treatment, wounds with surrounding skin were excised from treated mice 7 days after injury (day 6 after treatment). Sections from the central part of the wounds were stained with hematoxylin/eosin or Masson's trichrome and used for histological analysis. Computer-assisted morphometric analysis revealed that the granulation tissue area was significantly reduced in saline-treated diabetic mice with respect to healthy controls. Furthermore, AdCMV.PIGF, but not AdCMV.LacZ, treatment induced the formation of granulation tissue to an extension comparable with that observed in healthy mice (Figure 6A). Moreover, the morphological analysis of Masson's trichrome-stained sections revealed that the granulation tissue was more mature in AdCMV.PIGF-treated wounds compared with diabetic wounds. Indeed, in AdCMV.LacZ-treated wounds, and in saline solution-treated specimens, the wound bed was largely filled with fibrin or with a poorly cellularized, avascular granulation tissue containing a minimal amount of newly deposited collagen (Figure 6, B and C). On the other hand, in AdCMV.PIGF-treated wounds a well-vascularized granulation tissue mainly populated by fibroblasts and display-

ing a collagen-rich extracellular matrix completely filled the wound bed (Figure 6, D and E).

### *Granulation Tissue Vascularization Is Increased after AdCMV.PIGF Diabetic Wound Treatment*

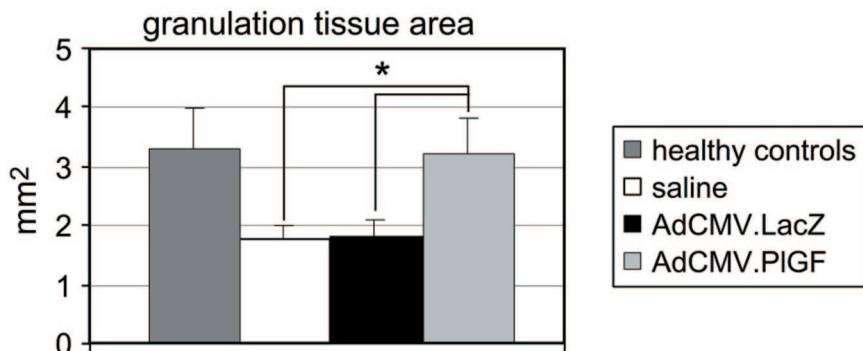
To quantify granulation tissue vascularization, an immunohistochemical analysis was performed on wound tissue specimens taken at day 7 after injury using an anti-PECAM/CD31 antibody. The computer-assisted morphometric analysis of the vasculature within the granulation tissue indicated that vascularization was significantly increased in AdCMV.PIGF-treated wounds with respect to both AdCMV.LacZ- and saline-treated ones (Figure 7). Specifically, PECAM/CD31-stained vessels were significantly more numerous and larger, as indicated by the higher number of vessels/mm<sup>2</sup>, the larger mean vessel area and the increased area covered by vessels in the granulation tissue (Figure 7, A–C).

Because PIGF has been reported to induce granulation tissue vessel maturation,<sup>4</sup> we also evaluated the density of vessels surrounded by pericytes/smooth muscle cells in the granulation tissue of wound specimens, by staining sections with an anti- $\alpha$ -SMA antibody. The number of vessels surrounded by a continuous SMA<sup>+</sup>-cell layer/mm<sup>2</sup> was significantly higher in the granulation tissue of AdCMV.PIGF-treated wounds compared with AdCMV.LacZ- and saline-treated controls (Figure 7, D–F). The density of SMA-positive vessels was comparable in AdCMV.PIGF-treated and healthy controls (Figure 7D). Of note, muscle cell-coated vessels in the granulation tissue of AdCMV.PIGF-treated diabetic mice represented 19.6% of PECAM/CD31-stained vessels, whereas in saline-treated and AdCMV.LacZ-treated diabetic wounds they were 2.9 and 5.0%, respectively. In healthy controls, SMA-positive vessels were 26.5% of the total vasculature within the granulation tissue.

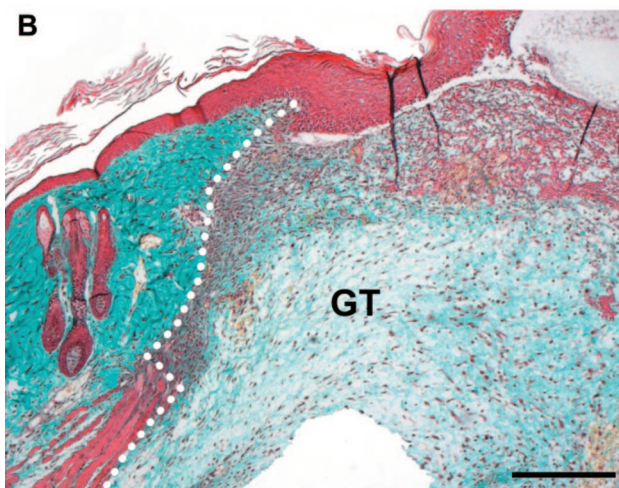
### *Inflammatory Cell Recruitment to the Wound Site Is Increased in Diabetic Mice Treated with AdCMV.PIGF*

To further characterize the biological effects exerted by PIGF transduction into the diabetic wounds, monocyte/macrophage recruitment was investigated. Sections of wound specimens collected at day 7 after injury were treated with an antibody against the Mac3 antigen and the number of labeled cells within the granulation tissue quantified by computer-assisted morphometric analysis. The results obtained indicate that monocyte/macrophage density was significantly reduced in the granulation tissue of diabetic mice with respect to healthy controls (Figure 8A). In the wounds treated with the AdCMV.PIGF, the number of monocytes/macrophages in the granulation tissue was increased compared with AdCMV.LacZ- and saline-treated controls, whereas no significant difference was observed in the number of Mac3-positive cells in AdCMV.PIGF-treated mice compared with healthy controls.

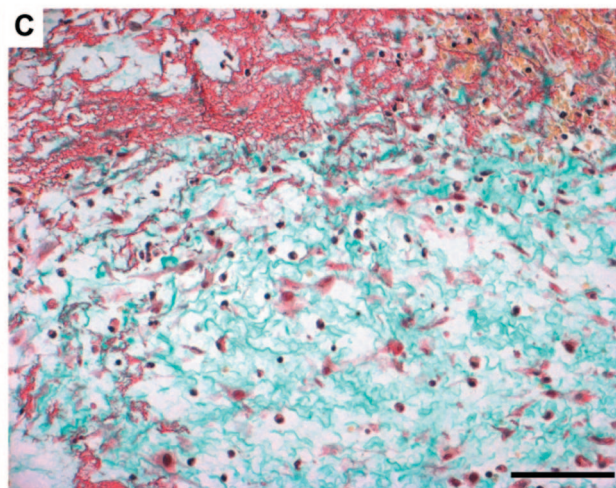
**A**



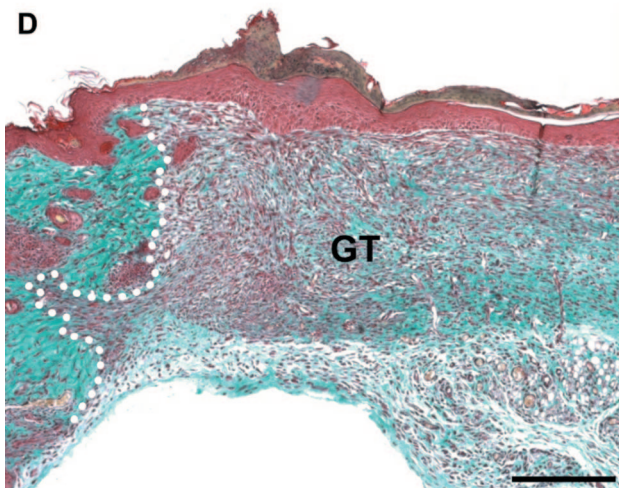
**B**



**C**



**D**



**E**

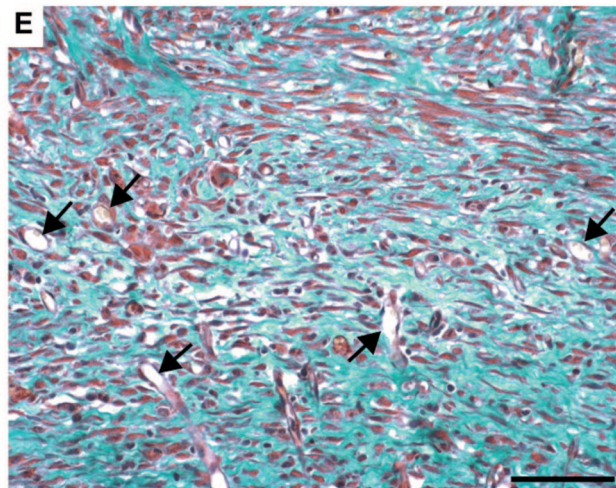


**Figure 6.** Effect of AdCMV.PIGF application on granulation tissue formation. **A:** Analysis of granulation tissue area in the central sections from wound specimens collected 7 days after wounding (6 days after treatment). The amount of granulation tissue is significantly increased in AdCMV.PIGF-treated wounds with respect to either AdCMV.LacZ- or saline-treated wounds and is similar to that present in healthy controls. \* $P < 0.05$ . **B–D:** Central sections of wounds treated with AdCMV.LacZ (**B**, lower magnification, and **C**, higher magnification) or AdCMV.PIGF (**D**, lower magnification, and **E**, higher magnification) collected 7 days after wounding (6 days after treatment) and stained with Masson's trichrome. In AdCMV.LacZ-treated wounds the granulation tissue (GT) is mainly filled with fibrin (red) or a poor collagen matrix (green) and contains few cells. In AdCMV.PIGF-treated wounds, a mature granulation tissue with abundant collagen deposition and containing numerous cells, in particular fibroblasts, and vessels (arrows) fill the wound bed. White dots indicate the boundary between the dermis and the granulation tissue. Scale bars: **B** and **D**, 250  $\mu\text{m}$ ; **C** and **E**, 75  $\mu\text{m}$ .

Because PIGF has been shown to mobilize/recruit bone marrow-derived hematopoietic stem cells,<sup>12</sup> we analyzed the presence of myeloid precursors in the peripheral blood of diabetic mice following wound treatments.

We first examined whether adenovirus-derived human PIGF could be detected in the blood stream. To this end, peripheral blood was collected from mice treated with AdCMV.PIGF and from control animals and human PIGF

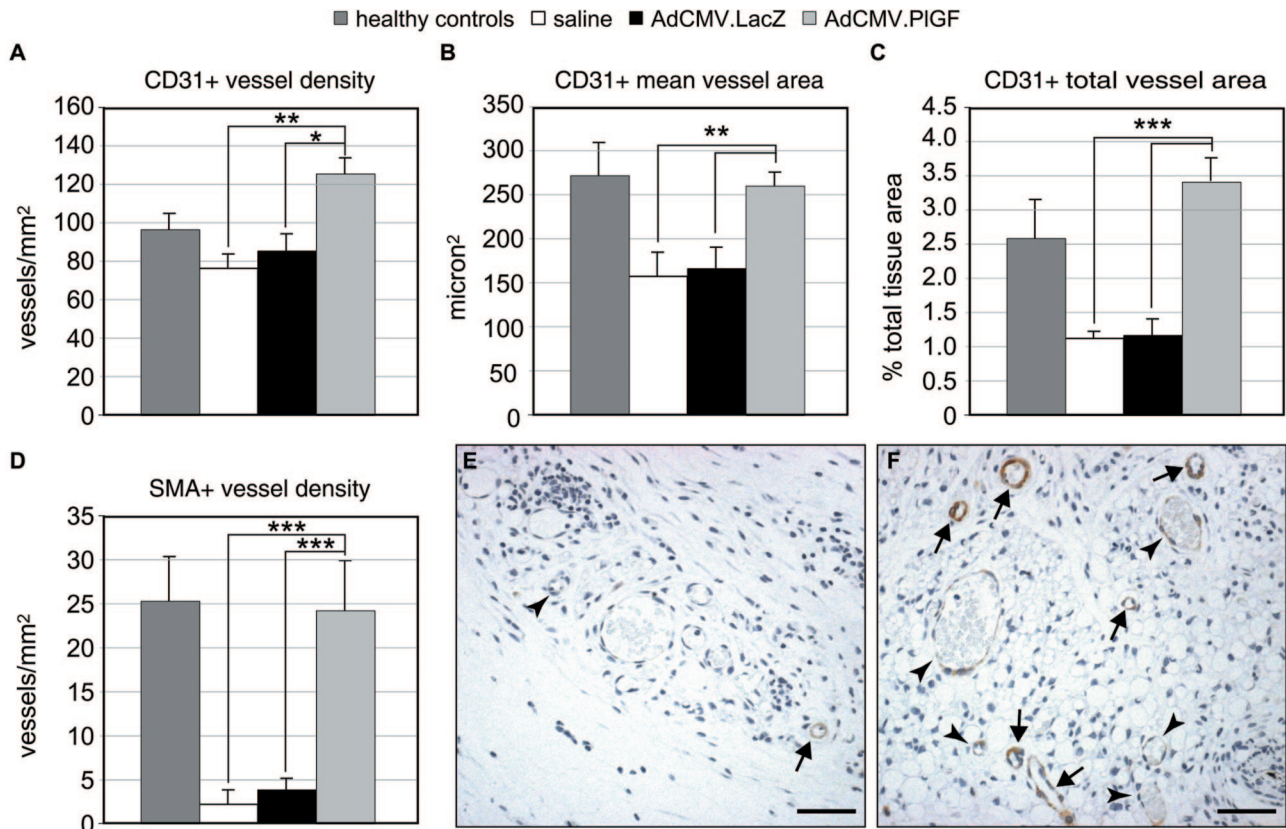


**Figure 7.** Analysis of granulation tissue vascularization. Central sections of wounds collected 7 days after wounding (6 days after treatment) were stained with an anti-PECAM/CD31 antibody or an anti- $\alpha$ -smooth muscle actin (SMA) antibody to detect endothelial cells and pericytes/smooth muscle cells, respectively. Vessel density (A, D), mean vessel area (B), and total area covered by vessels (C) were measured by computer-assisted morphometric analysis. In AdCMV.PIGF-treated diabetic specimens, total blood vessel density (A), mean vessel area (B), and the area covered by vessels (C) are significantly increased compared with both AdCMV.LacZ- and saline-treated diabetic wounds. In addition, the density of vessels surrounded by a continuous layer of SMA-positive cells is significantly increased in AdCMV.PIGF-treated wounds (D) ( $n = 6$ ). Values are expressed as mean  $\pm$  SEM. \* $P < 0.05$ ; \*\* $P < 0.01$ ; \*\*\* $P < 0.005$ . The differences between AdCMV.PIGF-treated and healthy control wounds are significant only for the vessel density ( $P < 0.05$ ). E and F: Representative fields of the granulation tissue of SMA-stained sections from AdCMV.LacZ-treated (E) and AdCMV.PIGF-treated (F) wounds, illustrating the increase in the density of "mature" vessels (arrows) in PIGF-transduced wounds. On the contrary, in AdCMV.LacZ-treated wounds the almost totality of vessels are not surrounded by a continuous layer of smooth muscle cells (arrowheads). Scale bars = 50  $\mu$ m.

concentration measured by ELISA on plasma samples. Human PIGF could be detected in the plasma of AdCMV.PIGF-treated mice collected 2, 4, and 7 days after treatment (ie, 3, 5, and 8 days after injury), at a concentration of  $45.61 \pm 26.6$ ,  $25.4 \pm 11.9$ , and  $36.61 \pm 13.9$  pg/ml, respectively, while undetectable in control animals (not shown).

Colony forming assays for myeloid precursors performed 2, 4, and 7 days after treatment (ie, 3, 5, and 8 days after injury) indicated that in mice treated with AdCMV.PIGF the number of colonies was not increased compared with mice treated with AdCMV.LacZ or saline solution (Figure 8B).

#### *Increased Expression of Growth Factors within the Wound Bed Following Adenovirus-Mediated PIGF Gene Transfer*

To investigate whether the beneficial effect exerted by AdCMV.PIGF treatment could be also mediated by up-regulation of growth factors involved in different aspects of wound healing, we analyzed by real-time RT-PCR the

mRNA levels of PDGF-B, TGF $\beta$ -1 and FGF-2 at different time points after AdCMV.PIGF application. In parallel, we analyzed the mRNA expression of VEGF, which is known to act synergistically with PIGF in inducing angiogenesis. The mRNA induction observed in wounds from healthy control animals was strongly decreased in the diabetic condition for all growth factors analyzed (Figure 9, A–D). PDGF-B, FGF-2 and VEGF showed a significant increase in the mRNA levels in the wounds of diabetic mice treated with AdCMV.PIGF with respect to AdCMV.LacZ-treated diabetic wounds. More specifically, PDGF-B and VEGF mRNA increase was highly significant at day 8 after treatment (5.5-fold increase for both growth factors) in the wounds treated with AdCMV.PIGF over AdCMV.LacZ-treated ones. Such increase was delayed in time and was stronger than that observed in wounds from healthy mice (Figure 9, A and D). FGF-2 induction was significantly higher in AdCMV.PIGF- over AdCMV.LacZ-treated diabetic wounds starting from day 4 after treatment and reaching a 4.3-fold difference at day 6, with timing and levels comparable with those observed in healthy wounds (Figure 9B). On the other hand, TGF $\beta$ -1 mRNA

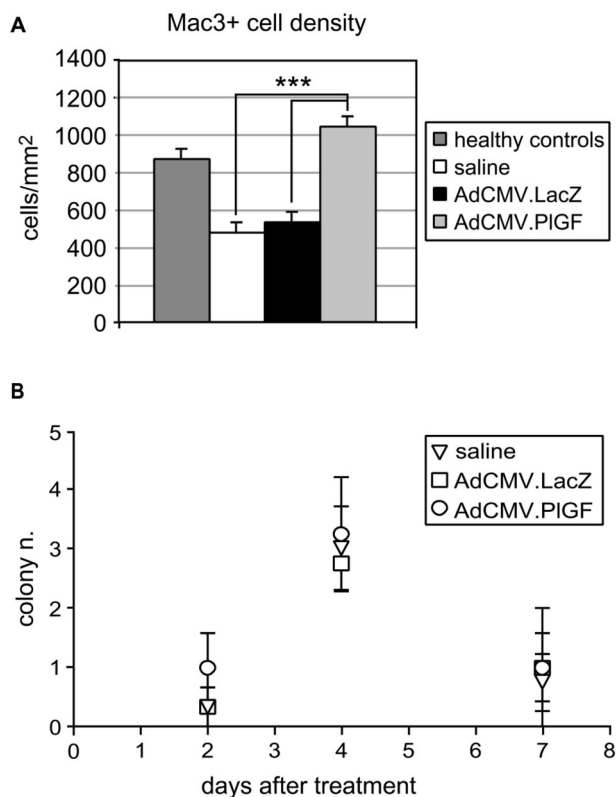


**Figure 8.** Monocyte/macrophage recruitment into the wound site and hematopoietic precursor mobilization in the peripheral blood. **A:** Computer-assisted analysis of Mac3-positive cells in the granulation tissue of wound specimens collected 7 days after wounding (6 days after treatments). The density of Mac-3-stained cells is significantly increased in AdCMV.PIGF-treated diabetic wounds compared with AdCMV.LacZ- and saline-treated diabetic wounds. The difference between AdCMV.PIGF-treated and healthy control wounds is not significant.  $***P < 0.005$ . **B:** Colony-forming assay of myeloid precursors isolated from the peripheral blood 2, 4, and 7 days after treatment. The number of colonies is similar in AdCMV.PIGF-, AdCMV.LacZ-, and saline-treated mice at all of the time points analyzed ( $n = 4$ ).

levels, normally peaking at day 3 after injury, were augmented following AdCMV.PIGF treatment with respect to saline treatment but to levels comparable with those observed in AdCMV.LacZ-treated wounds (Figure 9C).

### PIGF Treatment Enhances Cultured Dermal Fibroblast Migration

Granulation tissue maturation is strictly dependent on fibroblast proliferation and migration into the fibrin clot. To test whether PIGF could directly promote granulation tissue maturation by acting on fibroblasts, we first analyzed VEGFR-1 expression in cultured human dermal fibroblasts. RT-PCR using primers amplifying the intracellular tyrosine-kinase domain showed that VEGFR-1 is transcribed by dermal fibroblasts (Figure 10A). By RT-PCR we also checked for VEGFR-2 expression using primers amplifying the intracellular receptor region and found that the mRNA for this receptor is not transcribed in dermal fibroblasts (Figure 10A). The analysis by Western blotting on cell lysates confirmed that VEGFR-1, but not VEGFR-2, is expressed by cultured dermal fibroblasts (Figure 10B).

The effect of PIGF on fibroblast proliferation and migration was then examined. Fibroblast proliferation was analyzed in cells cultured for 24, 48, and 72 hours in the presence of different concentrations of human recombinant PIGF (from 10 to 100 ng/ml). A modest, although significant, increase in fibroblast proliferation was observed only in cells treated for 72 hours with 100 ng/ml PIGF (Figure 10C). FGF-2 treatment (10 ng/ml), used as a positive control, significantly stimulated fibroblast proliferation at all of the time points analyzed. On the other hand, PIGF enhanced fibroblast migration at all of the concentrations analyzed (from 25 to 100 ng/ml, data not shown) with a maximal increase of about 3.5-fold at a dose of 50 ng/ml (Figure 10D). Anti-PIGF or an anti-VEGFR-1 antibody treatment, but not anti-VEGF or an anti-VEGFR-2 administration, inhibited such effect. A comparable increase in cell migration was observed following stimulation with a mixture of insulin-transferrin-selenium selenite, used as a positive control, and such response was not affected by anti-PIGF or anti-VEGFR-1 antibody treatment (data not shown).

### Discussion

In this study we demonstrated that PIGF expression is strongly reduced during wound healing in an animal model of diabetes and that overexpression of this growth factor is able to accelerate wound closure in diabetic mice. We also show that PIGF gene transfer into diabetic mouse cutaneous wounds promotes repair by enhancing granulation tissue formation, maturation, and vascularization. Local recruitment of inflammatory cells and increased expression of growth factors, known to play a major role in wound repair, also follow adenovirus-driven PIGF expression. We finally show that PIGF directly stimulates cultured dermal fibroblast migration. All together our data confirm a role for PIGF in the wound healing process and indicate a therapeutic potential of this factor in defective skin repair.

PIGF is one of the proangiogenic molecules that are produced during wound healing. In the skin, this growth factor is expressed by keratinocytes and by endothelial cells, and such expression, which is extremely low in conditions of skin homeostasis, is up-regulated in association with both physiological and pathological neoangiogenesis.<sup>19–22</sup> The analysis of PIGF knockout mice indicated that PIGF expression is required to obtain an optimal wound healing and for granulation tissue vessel maturation.<sup>4</sup> Because PIGF up-regulation during wound healing temporarily coincides with VEGF one<sup>20,27</sup> and PIGF has been shown to potentiate VEGF proangiogenic function,<sup>4</sup> these two factors probably exert a synergistic action in the repair process.

The expression of VEGF was shown to be reduced in diabetic wounds.<sup>28</sup> VEGF administration results in accelerated re-epithelialization of diabetic wounds associated with enhanced vessel formation.<sup>23,29,30</sup> However, exogenous administration of VEGF induces sustained vascular leakage and promotes the formation of disorganized blood vessels as well as of malformed and poorly func-

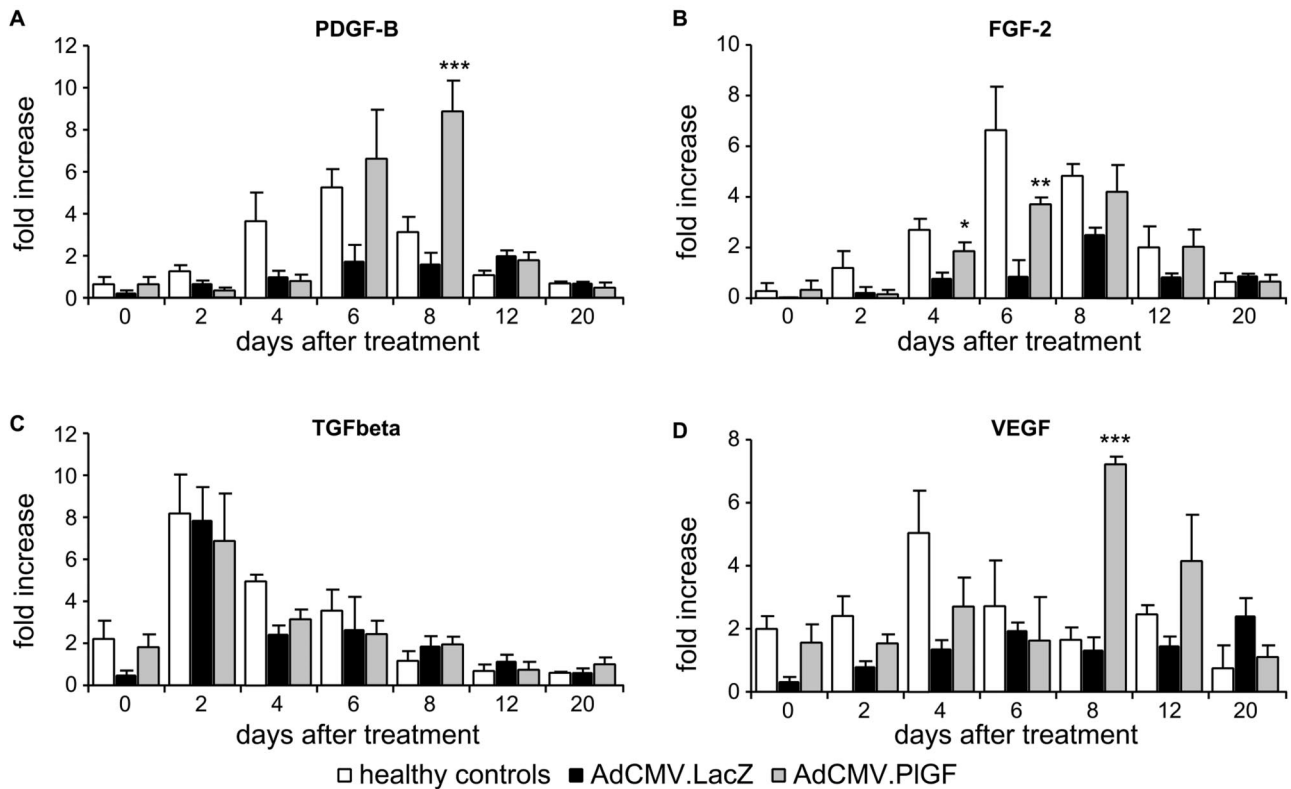


**Figure 9.** Increased transcription of growth factors playing a role in wound healing in AdCMV.PIGF-treated wounds. Real-time PCR analysis of PDGF-B (A), FGF-2 (B), TGF- $\beta$  (C), and VEGF (D) mRNA levels in the wounds of diabetic mice treated with AdCMV.LacZ, AdCMV.PIGF, and of nondiabetic healthy mice, expressed as fold increase over the amount of mRNA in saline-treated diabetic wounds ( $n = 3$ ). Values are expressed as mean  $\pm$  SEM. \* $P < 0.05$ ; \*\* $P < 0.01$ ; \*\*\* $P < 0.005$ .

tional lymphatic vessels.<sup>17,31</sup> These effects have raised concern on the use of VEGF in human therapy.

The observations that PIGF specifically enhances adult pathophysiological neovascularization,<sup>4</sup> does not interfere with lymphatic vessel function, and induces augmented permeability only when administered at high concentration<sup>17-18</sup> make it an attractive candidate for the therapeutic modulation of adult angiogenesis.

We, therefore, asked whether decreased PIGF expression may also contribute to diabetic wound healing impairment and whether PIGF overexpression could improve diabetic skin repair. We found that PIGF induction is strongly reduced in diabetic wounds. This decrease correlates with VEGFR-1 diminished expression that involves both the transmembrane and the soluble receptor isoform, as assessed by real-time RT-PCR. In particular, the mRNA levels for the soluble isoform are strongly reduced in the diabetic wounds, suggesting that this receptor, which is released by cells, does not contribute to the angiogenic impairment in the diabetic wounds by negatively modulating VEGF and/or PIGF action. By using transgenic mice overexpressing PIGF under the control of the keratin 14 promoter, we also showed that PIGF overexpression in basal keratinocytes only slightly improves wound healing in healthy mice without inducing a more rapid wound closure, whereas the improvement is marked in healing-impaired diabetic mice with an acceleration of the repair response. Such effect associates with enhanced granulation tissue vascularization, which is characterized by significantly larger vessels compared

with the wounds of diabetic wild-type mice, in keeping with the reported capacity of overexpressed PIGF to enhance vessel size.<sup>16,18</sup> These findings point to the involvement of PIGF in the altered healing process of pharmacologically induced diabetic mice and prompted us to test the therapeutic potential of PIGF in defective cutaneous wound healing. To this end, we analyzed skin repair in streptozotocin-induced diabetic mice, a model of type 1 diabetes. Surgical wounds performed in diabetic mice display a delayed and impaired healing and, although different under several aspects from diabetic chronic ulcers in humans, have been widely used as preclinical model to test the therapeutic potential of a number of growth factors.<sup>2</sup> In agreement with previous data in mouse models of heart and hindlimb ischemia,<sup>14,15</sup> we found that exogenous PIGF overexpression has therapeutic potential in wound healing. PIGF gene transfer significantly accelerates wound closure in diabetic mice, which heals at a rate similar to that observed in healthy control wounds.

In keeping with the results obtained in K14-PIGF diabetic mice and with the well-recognized role of PIGF as an angiogenic factor, the granulation tissue of the PIGF-transduced wounds shows increased vascularization with respect to control wounds. Both vessel density and vessel mean area are significantly enhanced following AdCMV.PIGF treatment. The difference in vessel density may be increased by the lack of newly forming vessels in extended portions of the granulation tissue in diabetic mice treated with the control vector or with saline solution.

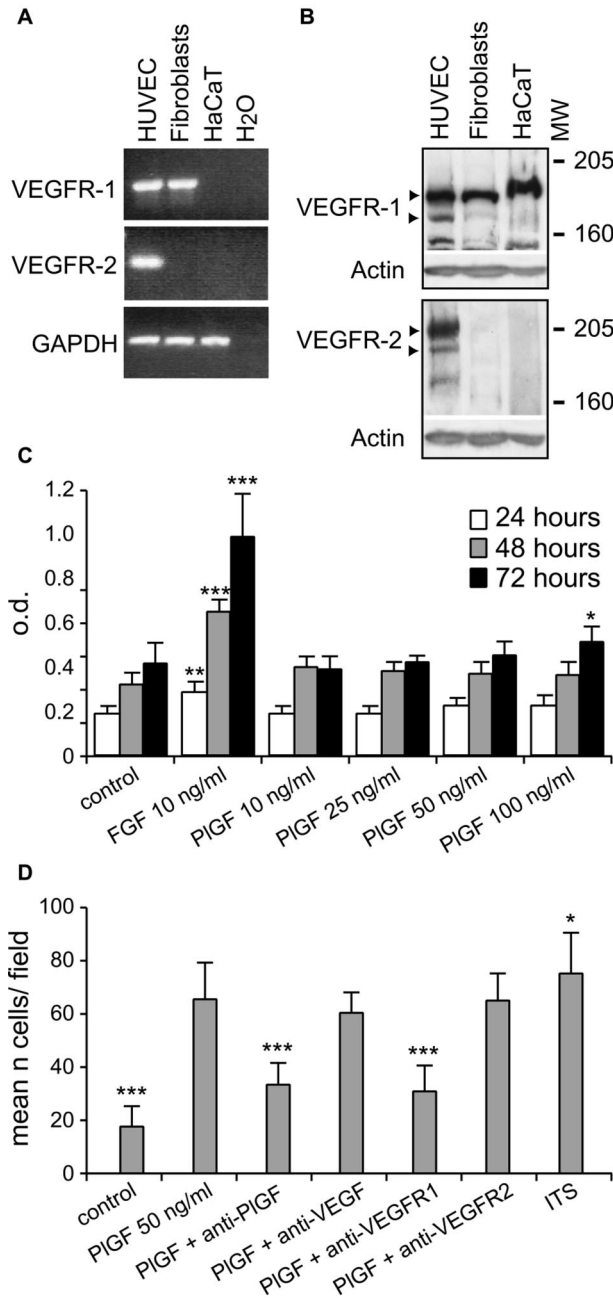


**Figure 10.** Expression of VEGFR-1 by cultured normal human dermal fibroblasts: proliferative and chemotactic responses to PIGF. **A:** RT-PCR analysis of VEGFR-1 and VEGFR-2 transcription by cultured dermal fibroblasts. Human umbilical vein endothelial cells have been used as a positive control and HaCaT keratinocyte cell line as a negative one. **B:** Western blot analysis for VEGFR-1 and VEGFR-2 confirms that VEGFR-1 is expressed by dermal fibroblasts, whereas VEGFR-2 is not. Human umbilical vein endothelial cells (HUVECs) have been analyzed as a positive control and HaCaT keratinocyte cell line as a negative one. **C:** Proliferation assay on dermal fibroblasts treated with PIGF at different concentrations and for different times. PIGF does not induce proliferation at all of the conditions tested apart from a slight, but a significant increase observed when cells are treated with the maximal concentration of the growth factor (100 ng/ml) for 72 hours. The effect of FGF-2 as positive control is shown. \* $P < 0.05$ ; \*\*\* $P < 0.001$ ; \*\*\*\* $P < 0.0005$  versus control. **D:** Migration of cultured dermal fibroblasts in response to PIGF. Compared with untreated cells, PIGF was able to induce fibroblast migration to an extent similar to that obtained by treating cells with a mixture of insulin-transferrin-sodium selenite (ITS), used as positive control. Anti-PIGF or an anti-VEGFR-1 antibody treatment inhibited such effect, which was not affected following anti-VEGF or anti-VEGFR-2 antibody treatment. \* $P < 0.05$ ; \*\*\*\* $P < 0.0005$  versus PIGF.

Indeed, these later animals show a strong delay in granulation tissue maturation compared with AdCMV.PIGF-treated wounds where blood vessels are homogeneously distributed within the wound bed.

We have shown that PIGF transduction in diabetic wounds also correlates with an increased number of vessels surrounded by pericytes/smooth muscle cells compared with control diabetic wounds. This finding indicates that PIGF-induced vasculature is functional. It also agrees with the reported PIGF arteriogenic activity<sup>11,32</sup> and with the observation that PIGF knockout mice delayed wound healing associates with reduced number of "mature" cell-coated vessels.<sup>4</sup>

The most striking effects exerted by PIGF gene expression are the increased formation and accelerated maturation of granulation tissue. Therefore, PIGF seems to promote not only vessel formation but also mature granulation tissue formation in AdCMV.PIGF-treated wounds. Among the different cell types contributing to granulation tissue formation, fibroblasts play a pivotal role. Fibroblasts invade the fibrin clot, the provisional matrix that is formed shortly after injury, and start to deposit a collagen-rich extracellular matrix, creating the condition for other cell types to migrate into the newly formed tissue and contributing to its further maturation. Endothelial cells temporally follow fibroblasts in this process. Together with other abnormalities, diabetic fibroblasts show a reduced migration capacity compared with normal fibroblasts.<sup>33</sup> We therefore at first investigated if the effect on granulation tissue formation and maturation could be mediated by an increased expression of growth factors, which are major players in the wound healing process and are specifically involved in enhancing fibroblast function. To this end, the transcription of PDGF-B, TGF $\beta$ , FGF-2, and VEGF was analyzed in diabetic wounds following adenovirus-mediated PIGF gene transfer and in controls. The induction of the mRNA for all factors is reduced in the diabetic wounds compared with healthy controls. Of the four factors, PDGF-B, FGF-2, and VEGF mRNA levels are increased following AdCMV.PIGF treatment. A similar effect on PDGF and FGF-2 has been reported by others after VEGF administration to wounds of genetically diabetic mice.<sup>23</sup> This preliminary analysis indicates that PIGF gene transfer may lead to accelerated wound closure in diabetic animals via the induction of other factors. Nevertheless, such induction is delayed with respect to the endogenous one in control healthy animals and follows the initial stages of granulation tissue formation. This finding suggests that the observed increase in the expression of the three factors may promote late healing events, rather than early ones.

Importantly, we could demonstrate that PIGF also exerts a direct effect on dermal fibroblasts. We show that these cells express VEGFR-1 but not VEGFR-2. We also demonstrate that fibroblasts migrate in response to PIGF treatment. VEGFR-1 is known to mediate chemotactic signals rather than proliferative ones,<sup>10,12,34</sup> it is therefore not surprising that we could observe only a minor induction in fibroblast proliferation by PIGF, although motility

was strongly increased following PIGF stimulation. The chemotactic effect was not affected by adding an anti-VEGF antibody and was also markedly reduced by an anti-VEGFR-1 antibody, indicating the PIGF directly stimulates fibroblast migration. Such an effect may be especially important in the process of granulation tissue formation and maturation that is, indeed, markedly accelerated in PIGF-transduced wounds.

Macrophages represent an important component of the inflammatory response that follows skin injury. Despite recent evidence indicates that wound healing is not delayed in mice lacking macrophages,<sup>35</sup> these cells are thought to give a significant contribution to skin repair by removing the cell debris and by producing a number of cytokines. In diabetic mice, the number of monocytes/macrophages is decreased compared with healthy controls. Because PIGF is a strong chemoattractant for VEGFR-1 expressing monocytes,<sup>10</sup> and the therapeutic activity of PIGF has been shown to be mediated by accumulation of activated monocytes/macrophages,<sup>11</sup> we examined this cell type in AdCMV.PIGF-treated wounds and in controls. We found that PIGF gene transfer is associated with an increased number of Mac3-positive cells in the wound bed. Such a finding suggests that enhanced macrophage recruitment leading to increased growth factor release may contribute to the accelerated healing observed in PIGF-transduced wounds. However, K14-PIGF diabetic mice show accelerated and improved wound closure associated with enhanced vascularization compared with wild-type diabetic littermates in the absence of increased macrophage recruitment. This finding indicates that at least part of the beneficial effects exerted by PIGF overexpression is not dependent on macrophage influx. With respect to macrophage recruitment, it is also important to note that the density of Mac3-positive cells in the granulation tissue of AdCMV.PIGF-treated diabetic wounds does not significantly exceed that of healthy controls. Indeed, the inflammatory response is required for optimal wound healing, but excessive and/or prolonged inflammation has negative effects on later stages of the healing process leading to abnormal scar formation. Scar formation is also associated to excess of granulation tissue. Diabetic mice show significantly reduced granulation tissue and PIGF gene transfer enhances the dimension of the granulation tissue to levels comparable with those of healthy wounds.

Despite PIGF has been shown to mobilize hematopoietic precursors in the peripheral blood,<sup>12</sup> we could not find any difference in the number of myeloid precursors in the blood of AdCMV.PIGF-treated mice with respect to controls at 2, 4, and 7 days after application. This result suggests that PIGF treatment in our experimental conditions exerts mainly a local effect. This interpretation is supported by the low amount of human PIGF detected in the blood of AdCMV.PIGF-treated mice (up to 45.61 pg/ml) compared with the levels of PIGF found in the peripheral blood of mice treated with recombinant PIGF for which an effect on the mobilization of hematopoietic precursors has been reported (10 ng/ml).<sup>12</sup> On the other

hand, because PIGF exerts a chemotactic effect on hematopoietic and endothelial progenitor cells, it cannot be excluded that local overexpression of this factor may enhance homing of circulating progenitor cells that are similarly mobilized in peripheral blood in AdCMV.LacZ- and AdCMV.PIGF-treated mice.

In conclusion, our data show a role for PIGF in impaired diabetic wound repair. They also indicate that PIGF gene transfer to diabetic wounds significantly accelerates closure, thus having therapeutic potential for diabetic ulcer treatment. PIGF gene transfer exerts its beneficial effect by directly and indirectly enhancing different aspects of the repair process, suggesting a wider spectrum of action for PIGF in the wound healing process not limited to its capacity to induce angiogenesis.

### Acknowledgments

We wish to thank Gabriele Toietta, Annalisa Antonini, and Silvia Truffa for adenovirus production, and Maurizio Inzillo for art work.

### References

1. Martin P: Wound healing-aiming for perfect skin regeneration. *Science* 1997, 276:75–81
2. Werner S, Grose R: Regulation of wound healing by growth factors and cytokines. *Physiol Rev* 2003, 83:835–870
3. Abaci A, Oguzhan A, Kahraman S, Eryol N, Unal S, Arinc H, Ergin A: Effect of diabetes mellitus on formation of coronary collateral vessels. *Circulation* 1999, 99:2239–2242
4. Carmeliet P, Moons L, Luttun A, Vincenzi V, Compernelle V, De Mol M, Wu Y, Bono F, Devy L, Beck H, Scholz D, Acker T, DiPalma T, Dewerchin M, Noel A, Stalmans I, Barra A, Blacher S, Vandendriessche T, Ponten A, Eriksson U, Plate KH, Foidart JM, Schaper W, Charnock-Jones DS, Hicklin DJ, Herbert JM, Collen D, Persico MG: Synergism between vascular endothelial growth factor and placental growth factor contributes to angiogenesis and plasma extravasation in pathological conditions. *Nat Med* 2001, 7:575–583
5. Park JE, Chen HH, Winer J, Houck KA, Ferrara N: Placenta growth factor. Potentiation of vascular growth factor bioactivity, *in vitro* and *in vivo*, and high affinity binding to Flt-1 but not to Flk-1/KDR. *J Biol Chem* 1994, 269:25646–25654
6. Maglione D, Guerriero V, Viglietto G, Ferraro M, Aprelikova O, Alitalo K, Del Vecchio S, Lei K, Chou J, Persico M: Two alternative mRNAs coding for the angiogenic factor, placenta growth factor (PIGF), are transcribed from a single gene of chromosome 14. *Oncogene* 1993, 8:925–931
7. Cao Y, Ji W-R, Qi P, Rosin A, Cao Y: Placenta growth factor: identification and characterization of a novel isoform generated by RNA alternative splicing. *Biochem Biophys Res Commun* 1997, 235:493–498
8. Migdal M, Huppertz B, Tessler S, Comforti A, Shibuya M, Reich R, Baumann H, Neufeld G: Neuropilin-1 is a placenta growth factor-2 receptor. *J Biol Chem* 1998, 273:22272–22278
9. Gluzman-Poltorak Z, Cohen T, Herzog Y, Neufeld G: Neuropilin-2 and neuropilin-1 are receptors for the 165-amino acid form of vascular endothelial growth factor (VEGF) and of placenta growth factor-2, but only neuropilin-2 functions as a receptor for the 145-amino acid form of VEGF. *J Biol Chem* 2000, 275:18040–18045
10. Clauss M, Weich H, Breier G, Knies U, Rockl W, Waltenberger J, Risau W: The vascular endothelial growth factor receptor Flt-1 mediates biological activities. Implication for a functional role of placenta growth factor in monocyte activation and chemotaxis. *J Biol Chem* 1996, 271:17629–17634
11. Pipp F, Heil M, Issbrucker K, Ziegelhoeffer T, Martin S, van de Heuvel J, Weich H, Fernandez B, Golomb G, Carmeliet P, Schaper W, Clauss

- M: VEGFR-1-selective VEGF homologue PIGF is arteriogenic. Evidence for a monocyte-mediated mechanism. *Circ Res* 2003, 92:378–385
12. Hattori K, Heissig B, Wu Y, Dias S, Tejada R, Ferris B, Hicklin DJ, Zhu Z, Bohlen P, Witte L, Hendriks J, Hackett NR, Crystal RG, Moore MA, Werb Z, Lyden D, Rafii S: Placental growth factor reconstitutes hematopoiesis by recruiting VEGFR1+ stem cells from bonemarrow microenvironment. *Nat Med* 2002, 8:841–849
  13. Autiero M, Waltenberger J, Communi D, Kranz A, Moons L, Lambrechts D, Kroll J, Plaisance S, De Mol M, Bono F, Kliche S, Fellbrich G, Ballmer-Hofer K, Maglione D, Mayr-Beyrle U, Dewerchin M, Dombrowski S, Stanimirovic D, Van Hummelen P, Dehio C, Hicklin DJ, Persico G, Herbert JM, Communi D, Shibuya M, Collen D, Conway EM, Carmeliet P: Role of PIGF in the intra- and intermolecular crosstalk between the VEGF receptors Flt-1 and Flk-1. *Nat Med* 2003, 9:936–943
  14. Lutun A, Tiwa M, Moons L, Wu Y, Angelillo-Scherrer A, Liao F, Nagy JA, Hooper A, Priller J, De Clerck B, Compornolle V, Daci E, Bohlen P, Dewerchin M, Herbert J-M, Fava R, Matthys P, Carmeliet G, Collen D, Dvorak HF, Hicklin DJ, Carmeliet P: Revascularization of ischemic tissues by PIGF treatment, and inhibition of tumor angiogenesis, arthritis and atherosclerosis by anti-Flt1. *Nat Med* 2002, 8:831–840
  15. Tamarat R, Silvestre J-S, Le Ricousse-Roussanne S, Barateau V, Lecomte-Raclet L, Clergue M, Duriez M, Tobelem G, Lévy BI: Impairment in ischemia-induced neovascularization in diabetes. Bone marrow mononuclear cell dysfunction and therapeutic potential of placenta growth factor treatment. *Am J Pathol* 2004, 164:457–466
  16. Odorisio T, Schietroma C, Zaccaria ML, Cianfarani F, Tiveron C, Tatangelo L, Failla CM, Zambruno G: Mice overexpressing placenta growth factor exhibit increased vascularization and vessel permeability. *J Cell Sci* 2002, 115:2559–2567
  17. Nagy JA, Vasile E, Feng D, Sundberg C, Brown LF, Detmar MJ, Lawitts JA, Benjamin L, Tan X, Manseau EJ, Dvorak AM, Dvorak HF: Vascular permeability factor/vascular endothelial growth factor induces lymphangiogenesis as well as angiogenesis. *J Exp Med* 2002, 196:1497–1506
  18. Nagy JA, Dvorak AM, Dvorak HF: VEGF-A164/165 and PIGF. Roles in angiogenesis and arteriogenesis. *Trends Cardiovasc Med* 2003, 13:169–175
  19. Cianfarani F, Zaccaria ML, Odorisio T, Zambruno G: Expression of placenta growth factor in mouse hair follicle cycle. *Gior Ital Dermatol Venereol* 140:497–503
  20. Failla CM, Odorisio T, Cianfarani F, Schietroma C, Puddu P, Zambruno G: Placenta growth factor is induced in human keratinocytes during wound healing. *J Invest Dermatol* 2000, 115:388–395
  21. Lacal PM, Failla CM, Pagani E, Odorisio T, Schietroma C, Falcinelli S, Zambruno G, D'Atri S: Human melanoma cells secrete and respond to placenta growth factor and vascular endothelial growth factor. *J Invest Dermatol* 2000, 115:1000–1007
  22. Graeven U, Rodeck U, Karpinski S, Jost M, Andre N, Schmiegel W: Expression patterns of placenta growth factor in human melanocytic cell lines. *J Invest Dermatol* 2000, 115:118–123
  23. Galiano RD, Tepper OM, Pelo CR, Bhatt KA, Callaghan M, Bastidas N, Bunting S, Steinmetz HG, Gurtner GC: Topical vascular endothelial growth factor accelerates diabetic wound healing through increased angiogenesis and by mobilizing and recruiting bone marrow-derived cells. *Am J Pathol* 2004, 164:1935–1947
  24. Pfaffl M: A new mathematical model for relative quantification in real time RT-PCR. *Nucl Ac Res* 2001, 29:2002–2007
  25. Gimbrone MA: Culture of vascular endothelium. *Prog Hemost Thromb* 1976, 3:1–28
  26. Kendall RL, Thomas KA: Inhibition of vascular endothelial cell growth factor activity by an endogenously encoded soluble receptor. *Proc Natl Acad Sci USA* 1993, 90:10705–10709
  27. Brown LF, Yeo K-T, Berse B, Yeo T-K, Senger DR, Dvorak HF, Van De Water L: Expression of vascular endothelial growth factor (vascular endothelial growth factor) by epidermal keratinocytes during wound healing. *J Exp Med* 1992, 176:1375–1379
  28. Frank S, Hubner G, Breier G, Longaker MT, Greenhalgh DG, Werner S: Regulation of vascular endothelial growth factor expression in cultured keratinocytes: implications for normal and impaired wound healing. *J Biol Chem* 1995, 270:12607–12613
  29. Romano Di Peppe S, Mangoni A, Zambruno G, Spinetti G, Melillo G, Napolitano M, Capogrossi MC: Adenovirus-mediated VEGF165 gene transfer enhances wound healing by promoting angiogenesis in CD1 diabetic mice. *Gene Ther* 2002, 9:1271–1277
  30. Deodato B, Arsic N, Zentilin L, Galeano M, Santoro D, Torre V, Altavilla D, Valdembrì D, Bussolino F, Squadrito F, Giacca M: Recombinant AAV vector encoding human VEGF165 enhances wound healing. *Gene Ther* 2002, 9:777–785
  31. Carmeliet P: VEGF gene therapy: stimulating angiogenesis or angioma-genesis? *Nat Med* 2000, 6:1102–1103
  32. Li W, Shen W, Gill R, Corbly A, Jones B, Belagaje R, Zhang Y, Tang S, Chen Y, Zhai Y, Wang G, Wagle A, Hui K, Westmore M, Hanson J, Chen Y, Simons M, Singh JP: High-resolution quantitative computed tomography demonstrating selective enhancement of medium-size collaterals by placenta growth factor-1 in the mouse ischemic hind-limb. *Circulation* 2006, 2445–2453
  33. Lerman OZ, Galiano RD, Armour M, Levine JP, Gurtner GC: Cellular dysfunction in the diabetic fibroblasts. Impairment of migration, vascular endothelial growth factor production, and response to hypoxia. *Am J Pathol* 2003, 162:303–312
  34. Fiedler J, Leucht F, Waltenberger J, Dehio C, Brenner RE: VEGF-A and PIGF-1 stimulate chemotactic migration of human mesenchymal progenitor cells. *Biochem Biophys Res Commun* 2005, 334:561–568
  35. Martin P, D'Souza D, Martin J, Grose R, Cooper L, Maki R, McKercher SR: Wound healing in the PU. 1 null mouse-tissue repair is not dependent on inflammatory cells. *Curr Biol* 2003, 13:1122–1128